IEEE Access
Multidisciplinary | Rapid Review | Open Access Journal

Received 27 September 2024, accepted 7 October 2024, date of publication 10 October 2024, date of current version 22 October 2024.

Digital Object Identifier 10.1109/ACCESS.2024.3477975

RESEARCH ARTICLE

A Novel Method Based on Sequential Unconstrained Programming for Transmit Beamforming in Colocated MIMO Radars

ELAHE FAGHAND[1,2], GIORGIO GUERZONI[1], ESFANDIAR MEHRSHAHI[2], GIORGIO MATTEO VITETTA[1], (Senior Member, IEEE), AND SHOKROLLAH KARIMIAN[2]

[1]Department of Engineering "Enzo Ferrari," University of Modena and Reggio Emilia, 41124 Modena, Italy
[2]Faculty of Electrical Engineering, Shahid Beheshti University, Tehran 19839-69411, Iran

Corresponding author: Elahe Faghand (elahe.faghand@unimore.it)

ABSTRACT The design of the waveform covariance matrix for beampattern matching in colocated *multiple-input multiple-output* (MIMO) radars represents a challenging problem because of its large number of variables and the presence of multiple constraints. The solutions available in the technical literature are computationally intensive and usually rely on iterative procedures that minimize a constrained *mean square error* (MSE). In this manuscript, a new computationally efficient method for beampattern matching design is proposed. This method, called *sequential weight-shift unconstrained programming* (SWSUP), allows to compute the covariance matrix of the probing signals achieving a desired beampattern at the transmit side of a colocated MIMO radar. Its derivation is based on the idea of reformulating the beampattern matching problem in an unconstrained form that can be tackled by breaking it into two subproblems. The first subproblem admits a closed-form solution, whose accuracy, in terms of MSE, is comparable to provided by other known methods. The solution of the second subproblem, instead, is evaluated through an iterative procedure and allows to achieve further improvement. Our numerical results evidence that the SWSUP method achieves precise beampattern matching with a substantially lower computational effort and computing time with respect to various existing alternatives.

INDEX TERMS Colocated multiple-input multiple-output radar, covariance matrix design, transmit beampattern matching, unconstrained programming.

I. INTRODUCTION

Colocated *multiple-input multiple-output* (MIMO) radars, thanks to their capability to radiate different probing waveforms from distinct antennas, can provide significant advantages, in terms of target identifiability, overall degrees of freedom and waveform diversity, with respect to radars equipped with phased arrays [1], [2], [3]. In principle, the full exploitation of the potentialities offered by a MIMO radar requires the joint design of its transmitted waveforms and *receive* (RX) filters. This should aim at properly adjusting the distribution of its radiated power and maximizing its output *signal-to-interference-plus-noise ratio* (SINR) under specific constraints; such constraints include the *constant modulus* (CM) or the *peak-to-average power ratio* (PAPR) constraint, and the *similarity* constraint [4], [5], [6], [7]. The design of the radiated waveforms represents a fundamental problem, since it influences the *transmit* (TX) beampattern [8]. In fact, a proper selection of the TX waveforms allows to radiate different amounts of power along distinct directions [9], [10] and, in particular, to: a) minimize the *mean squared error* (MSE) between a desired beampattern and the achieved one; b) minimize the *sidelobe level* (SLL) along those directions where no power is needed [11], [12]; c) insert deep nulls along specific directions. These results can be achieved by adopting a *direct* or an *indirect* approach to waveform design. On the one hand, the aim of *direct* waveform design is to evaluate the

The associate editor coordinating the review of this manuscript and approving it for publication was Zaharias D. Zaharis.

set of waveforms feeding each antenna without intermediate steps [13]. On the other hand, that of *indirect* waveform design is to compute first the *covariance matrix* relating the waveforms radiated by each antenna and, secondly, to synthesize the waveforms matching that matrix [14]. Both the aforementioned approaches are challenging because of their specific constraints. In fact, the waveforms resulting from direct design should satisfy the CM constraint in order to maximize the efficiency of their power amplification. The covariance matrix generated in indirect design, instead, is required to be *positive semidefinite* (PSD); moreover, all its main diagonal elements should be equal to ensure the same power level is radiated by each of the TX antennas.

In the technical literature, various strategies have been developed to design the radar waveforms and their covariance matrix. As far as direct waveform design is concerned, here we limit to mention: a) the use of independent finite-alphabet constant-envelope waveforms, such as *binary-phase-shift-keying* (BPSK) or *quadrature-phase-shift-keying* (QPSK), to minimise the MSE or the SLL [15], [16], [17], [18], [19]; b) the adoption of a residual neural network to minimize the MSE [20], [21]; c) the exploitation of various implementations of the *alternating direction method of multipliers* (ADMM) to minimize the MSE or the SLL [22], [23], [24], [25], [26].

Various methods have been also proposed to generate a proper covariance matrix for the radiated waveforms. In particular, the following results deserve to be mentioned: a) the use of convex optimization toolboxes (e.g., CVX [27], [28]) for the generation of a covariance matrix satisfying specific constraints and minimizing the MSE and the SLL, or introducing deep nulls in specific directions [29], [30], [31]; b) a method based on the *discrete Fourier transform* (DFT) for the synthesis of the covariance matrix in [32], [33]; c) a closed-form solution[1] for the covariance matrix minimising the MSE has been derived [34]. Unluckily, most of the direct and indirect methods available in the literature are not based on closed-form expressions and requires solving *constrained* optimization problems through iterative methods.

In this manuscript, a novel method for the design of the TX covariance matrix, called *sequential weight-shift unconstrained programming* (SWSUP), is illustrated. This method results from solving an unconstrained MSE minimization problem under the assumption that the desired beampattern can be approximated as a *sum* of *weighted* and *shifted* replicas of a proper basis beampattern,[2] having a known covariance matrix. This allows us to derive a closed-form solution for the optimal set of the weights of the components and to develop an iterative procedure optimizing their shifts; such a procedure can be initialised easily and its initial point represents a good approximation of the required shifts. The main features of the proposed method can be summarized as follows:

1) It does not require the use of complicated optimization tools.
2) It produces a covariance matrix satisfying practical constraints.
3) It can approximate any kind of beampattern (symmetric, asymmetric, singlelobe and multilobe) by minimising the associated MSE.

The remaining part of this manuscript is organized as follows. The model of the considered radar system and relevant signals is illustrated in Section II. The SWSUP method is derived and compared with various alternatives available in the technical literature in Section III. The SWSUP accuracy is assessed in Section IV, where the synthesis of specific beampatterns based on it and other methods is analysed. Finally, some conclusions are offered in Section V.

Notation: Bold upper case letters and bold lower case letters are employed to denote *matrices* and *vectors*, respectively. The symbols $(\cdot)^H$ and $(\cdot)^T$ denote *conjugate transposition* and *transposition*, respectively, of a matrix, whereas $\mathrm{E}\{\cdot\}$ denotes *statistical expectation*. The (m,n)th element of a matrix $\mathbf{X}$ is denoted $X_{m,n}$. The notation $\mathbf{X} > 0$ denotes that the matrix $\mathbf{X}$ is PSD. The notations $\mathbf{I}_M$ and $\mathbf{1}_{M,M}$ denote the $M \times M$ *identity matrix* and matrix having all its elements equal to one, respectively. The symbols $\odot$, $\oslash$ and $(\cdot)^{\circ 2}$ indicate elementwise multiplication, division and second power. The symbol $\lceil\cdot\rceil$ denotes the *ceiling function*.

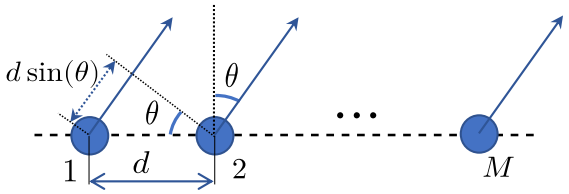

FIGURE 1. Representation of the considered ULA configuration.

II. SYSTEM AND SIGNAL MODELS

In the remaining part of this manuscript we focus on a colocated and monostatic MIMO radar system operating in a *two-dimensional* (2D) scenario and having the following properties:

1) It is equipped with a *uniform linear array* [3] (ULA), consisting of M calibrated antennas (see Fig. 1); the spacing between adjacent antennas, denoted d, is equal $\lambda/2$, where λ denotes the wavelength of all the radiated waveforms.
2) Its TX antennas simultaneously transmit narrowband signals.

[1] Note that the performance achievable through this solution gets worse in the case of asymmetric and multilobe patterns.

[2] Such replicas are called *components* from now on.

[3] Note that this is a standard assumption in the literature on beampatterm pattern design. If a different configuration is taken into consideration for the antenna array, the evaluation of the associated beampattern and its derivatives can become very complicated.

Let $x_m(n)$ denote the nth sample of the complex envelope of the probing signal radiated by the mth TX antenna (with $m = 1, 2, \ldots, M$). Then, in a nondispersive propagation scenario, the nth sample $y(n)$ of the complex envelope of the baseband signal impinging on a point target characterized by the azimuth θ can be expressed as[4] (e.g., see [29], eq.(1))

$$y(n) = \sum_{m=1}^{M} x_m(n) \exp(-j2\pi f_0 \tau_m(\theta)) \triangleq \mathbf{a}^H(\theta)\mathbf{x}(n), \quad (1)$$

with $n = 1, 2, \ldots, N$; here, f_0 represents the carrier frequency of all the radiated signals, N is the overall number of samples available in the considered observation interval,

$$\mathbf{x}(n) \triangleq [x_1(n), x_2(n), \ldots, x_M(n)]^T \quad (2)$$

is an M-dimensional complex vector collecting the nth samples of the all the transmitted signals,

$$\mathbf{a}(\theta) \triangleq [1, \exp(j\pi \sin(\theta)), \ldots, \exp(j\pi(M-1)\sin(\theta))]^T \quad (3)$$

is the M-dimensional *steering vector* of the radar array,

$$\tau_m(\theta) \triangleq \frac{(m-1)d\sin(\theta)}{c}, \quad (4)$$

represents the difference in the propagation delay between the leftmost antenna and the mth antenna of the ULA (e.g., see [35], eq. (6.2.22)), and c is the speed of light. Then, the average power $P(\theta)$ radiated by the radar system along the azimuth θ, i.e. the so called *transmit beampattern* , can be expressed as

$$\begin{aligned} P(\theta) \triangleq \mathrm{E}\left\{|y(n)|^2\right\} &= \mathrm{E}\{\mathbf{a}^H(\theta)\mathbf{x}(n)\mathbf{x}^H(n)\mathbf{a}(\theta)\} \\ &= \mathbf{a}^H(\theta)\mathbf{R}\,\mathbf{a}(\theta), \end{aligned} \quad (5)$$

where $\mathbf{R} \triangleq \mathrm{E}\{\mathbf{x}(n)\mathbf{x}^H(n)\}$ is the $M \times M$ covariance matrix characterizing the transmitted waveforms. From the last result, it is easily inferred that the design of a given beampattern can be reformulated as the problem of properly selecting the covariance matrix $\mathbf{R}$. In tackling the last problem, the following two practical constraints are usually set on $\mathbf{R}$ [29]:

1) This matrix is required to be PSD.
2) The elements along its main diagonal are required to be all equal, i.e.

$$R_{m,m} = \frac{\rho}{M} \quad (6)$$

for any $m = 1, \ldots, M$, where ρ denotes the overall power radiated by the radar array.

Provided that both practical constraints are met, the covariance matrix $\mathbf{R}$ should be synthesized in a way that the MSE between the desired beampattern and the resulting one is minimized.

[4]Note that: a) the pathloss for the radiated waveforms is ignored for simplicity; b) the propagation delay from the radar to the target can be neglected thanks to the narrowband assumption.

III. DERIVATION OF THE SWSUP METHOD

This section is devoted to the development of the SWSUP method and its comparison with other technical alternatives.

A. BEAMPATTERN SHIFTING

An important role in the derivation of the SWSUP method is played by the concept of *beampattern shifting* , i.e. by shifting a beampattern associated with a given covariance matrix; this subsection is devoted to explaining it. To begin, we define the auxiliary variable

$$\gamma \triangleq \sin(\theta) \quad (7)$$

and rewrite (3) and (5) as

$$\mathbf{a}(\gamma) = [1, \exp(j\pi\gamma), \ldots, \exp(j\pi(M-1)\gamma)]^T \quad (8)$$

and

$$P(\gamma) = \mathbf{a}^H(\gamma)\mathbf{R}\,\mathbf{a}(\gamma) \quad (9)$$

respectively. Inserting a *shift term* η, defined in the γ domain, in the transmit beampattern $P(\gamma)$ (9) produces

$$P(\gamma - \eta) = \mathbf{a}^H(\gamma - \eta)\mathbf{R}\,\mathbf{a}(\gamma - \eta). \quad (10)$$

If we define now the $M \times M$ matrix

$$\mathbf{A}(\eta) \triangleq \begin{bmatrix} 1 & 0 & \ldots & 0 \\ 0 & \exp(j\pi\eta) & \ldots & 0 \\ \vdots & \vdots & \ddots & \vdots \\ 0 & 0 & \ldots & \exp(j\pi(M-1)\eta) \end{bmatrix}, \quad (11)$$

then (10) can be rewritten as

$$P(\gamma - \eta) = \mathbf{a}^H(\gamma)\mathbf{A}(\eta)\mathbf{R}\,\mathbf{A}^H(\eta)\mathbf{a}(\gamma). \quad (12)$$

Based on the last result it is not difficult to prove that replacing the covariance matrix $\mathbf{R}$ with

$$\mathbf{R}^{(\mathrm{S})} \triangleq \mathbf{A}(\eta)\mathbf{R}\,\mathbf{A}^H(\eta) \quad (13)$$

in (5) produces a new beampattern, denoted $P^{(\mathrm{S})}(\gamma, \eta)$ and representing a shifted version of $P(\gamma)$, since

$$P^{(\mathrm{S})}(\gamma, \eta) = P(\gamma - \eta). \quad (14)$$

It is worth pointing out that:

1) The matrix $\mathbf{R}^{(\mathrm{S})}$ (13) satisfies the same constraints as $\mathbf{R}$.
2) A shift η in the γ domain is *not* equivalent to a shift in the θ domain, because of the nonlinear relationship (7). This concept is exemplified by Fig. 2, in which a specific beampattern and its shifted version in both the γ domain and the θ domain are shown.

In the remaining part of this section, we always refer to the γ domain in place of the θ domain, unless differently stated.

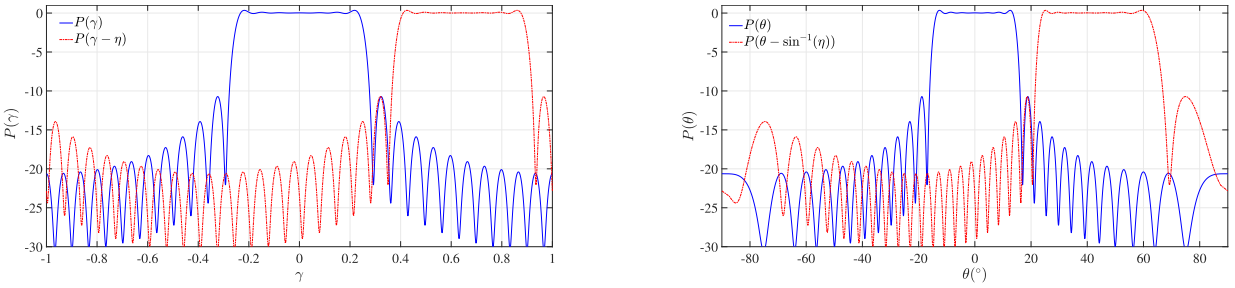

FIGURE 2. Representation of: a) a specific beampattern and its shifted version in the γ domain (a shift by $\eta = 0.64$, corresponding to 40°, is considered); b) the same beampatterns in the θ domain.

B. BEAMPATTERN MATCHING DESIGN

In this subsection, our approach to the problem of beampattern matching design is illustrated and a novel solution is developed. To begin, we define the covariance matrix

$$\mathbf{R}_0 \triangleq \mathbf{1}_{M,M}, \tag{15}$$

dubbed *basis covariance matrix* . This matrix has the following properties:

1)The beampattern associated with it corresponds to that of a uniform array having size M and a uniform feed. This array has the highest directivity (more precisely, the least half power beam width).

2) Its absolute maximum is achieved at $\gamma = 0$ (or, equivalently, at $\theta = 0$; see (7)).

3) All the components associated with this covariance matrix take the form[5]

$$P^{(\mathrm{S})}(\gamma,\eta) = \frac{1}{M^2}\left(\frac{\sin\left(M\frac{\pi}{2}(\gamma-\eta)\right)}{\sin\left(\frac{\pi}{2}(\gamma-\eta)\right)}\right)^2. \tag{16}$$

Let $P^{(\mathrm{D})}(\gamma)$ represent the function describing our desired beampattern; in the following, we assume that $P^{(\mathrm{D})}(\gamma) = 1$ for all those directions along which the electromagnetic energy has to be radiated by the TX antenna array and $P^{(\mathrm{D})}(\gamma) = 0$ elsewhere. Under these assumptions, our target consists in evaluating the covariance matrix $\hat{\mathbf{R}}^{(\mathrm{L})}$ that maximizes the power radiated along those directions for which $P^{(\mathrm{D})}(\gamma) = 1$ and minimizes the power elsewhere. To simplify this optimization problem, we make the following two choices:

1) We restrict the search for $\hat{\mathbf{R}}^{(\mathrm{L})}$ to the infinite set of matrices that can be put in the from

$$\mathbf{R}^{(\mathrm{L})}(\tilde{\mathbf{b}},\tilde{\mathbf{h}}) = \frac{1}{\tilde{I}}\sum_{i=1}^{\tilde{I}}\tilde{\beta}_i\mathbf{A}(\tilde{\eta}_i)\mathbf{R}_0\left(\mathbf{A}(\tilde{\eta}_i)\right)^H, \tag{17}$$

i.e., that can be expressed as a linear combination of $\tilde{I}$ shifted and scaled versions of the basis covariance matrix; here, $\tilde{\beta}_i$ and $\tilde{\eta}_i$ are the *weight* and *shift* , respectively, to be applied to $\mathbf{R}_0$ to generate the ith member of the representation (17) (with $i = 1, 2, \ldots, \tilde{I}$), and $\tilde{\mathbf{b}}$ and $\tilde{\mathbf{h}}$ are $\tilde{I}$-dimensional row vectors collecting the weights $\{\tilde{\beta}_i\}$ and shifts $\{\tilde{\eta}_i\}$, respectively.

2) We fix a set of K *directions of interest* $\{\gamma_k; k = 1, 2, \ldots, K\}$ along which the desired beampattern and the one associated with $\mathbf{R}^{(\mathrm{L})}(\tilde{\mathbf{b}},\tilde{\mathbf{h}})$ (17) (and denoted $P^{(\mathrm{S})}(\gamma,\eta)$) are compared.

In addition, we assign the positive weight ω_k to the beampattern corresponding to the kth direction of interest (with $k = 1, 2, \ldots, K$). Then, for a given $\tilde{I}$, the evaluation of $\hat{\mathbf{R}}^{(\mathrm{L})}$ can be formulated as the problem of searching for the matrix $\mathbf{R}^{(\mathrm{L})}(\tilde{\mathbf{b}},\tilde{\mathbf{h}})$ (17) that minimizes the MSE

$$e(\tilde{\mathbf{b}},\tilde{\mathbf{h}}) \triangleq \frac{1}{K}\left(\mathbf{v}\odot\left(\mathbf{p}^{(\mathrm{D})} - \mathbf{p}^{(\mathrm{L})}(\tilde{\mathbf{b}},\tilde{\mathbf{h}})\right)\right)^T \left(\mathbf{v}\odot\left(\mathbf{p}^{(\mathrm{D})} - \mathbf{p}^{(\mathrm{L})}(\tilde{\mathbf{b}},\tilde{\mathbf{h}})\right)\right). \tag{18}$$

In the last formula we have that:

1) $\mathbf{p}^{(\mathrm{D})}$ is the K-dimensional column vector containing the samples of the desired beampattern evaluated at the directions of interest $\{\gamma_k\}$; therefore, its kth element is defined as

$$p_k^{(\mathrm{D})} \triangleq P^{(\mathrm{D})}(\gamma_k), \tag{19}$$

with $k = 1, 2, \ldots, K$.

2) $\mathbf{p}^{(\mathrm{L})}(\tilde{\mathbf{b}},\tilde{\mathbf{h}})$ is the K-dimensional column vector containing the samples of the trial beampattern associated with the matrix $\mathbf{R}^{(\mathrm{L})}(\tilde{\mathbf{b}},\tilde{\mathbf{h}})$ (17) and evaluated at the directions of interest $\{\gamma_k\}$; this vector can be expressed as

$$\mathbf{p}^{(\mathrm{L})}(\tilde{\mathbf{b}},\tilde{\mathbf{h}}) = \mathbf{P}(\tilde{\mathbf{h}})\tilde{\mathbf{b}}^T, \tag{20}$$

where $\mathbf{P}(\tilde{\mathbf{h}}) = [P_{k,i}]$ is a $K \times I$ matrix, with

$$P_{k,i} \triangleq P^{(\mathrm{S})}(\gamma_k,\eta_i) \tag{21}$$

for $k = 1, 2, \ldots, K$ and $i = 1, 2, \ldots, \tilde{I}$.

3) The K-dimensional vector $\mathbf{v}$ is defined as

$$\mathbf{v} \triangleq [\sqrt{\omega_1}, \sqrt{\omega_2}\ldots, \sqrt{\omega_K}]^T. \tag{22}$$

Then, for a given $\tilde{I}$, $\hat{\mathbf{R}}^{(\mathrm{L})}$ is evaluated as

$$\hat{\mathbf{R}}^{(\mathrm{L})} = \mathbf{R}^{(\mathrm{L})}(\hat{\mathbf{b}},\hat{\mathbf{h}}) \tag{23}$$

where

$$\hat{\mathbf{b}},\hat{\mathbf{h}} = \arg\min_{\tilde{\mathbf{b}},\tilde{\mathbf{h}}}\left\{e(\tilde{\mathbf{b}},\tilde{\mathbf{h}})\right\}. \tag{24}$$

[5]See Appendix A for additional details.

Unluckily, this optimization problem does not admit a closed-form solution. For this reason, we resort to an iterative method based on *alternating minimization* . Its vth iteration (with $v = 1, 2, \ldots, V$, where V denotes the overall number of iterations) is fed by the estimates $\mathbf{h}^{(v-1)}$ and $\mathbf{b}^{(v-1)}$ of $\hat{\mathbf{b}}$ and $\hat{\mathbf{h}}$, respectively, made available by the previous iteration and generates the new estimates

$$\mathbf{b}^{(v)} = \arg\min_{\tilde{\mathbf{b}}} \left\{ e\left(\tilde{\mathbf{b}}, \mathbf{h}^{(v-1)}\right)\right\} \tag{25}$$

and

$$\mathbf{h}^{(v)} = \arg\min_{\tilde{\mathbf{h}}} \left\{ e\left(\mathbf{b}^{(v)}, \tilde{\mathbf{h}}\right)\right\}. \tag{26}$$

In the following, the optimization problems (25) and (26) are called *weight evaluation* and *shift evaluation* , respectively. Note that:

1) The iterative procedure defined above requires the knowledge of the initial estimate $\mathbf{h}^{(0)}$ (see (25)).

2) It can be stopped when the resulting MSE (see (18)) drops below a given threshold or after that a fixed number of iterations (say, V iterations) has been carried out; in the last case, we set

$$\hat{\mathbf{b}} = \mathbf{b}^{(V)} \tag{27}$$

and

$$\hat{\mathbf{h}} = \mathbf{h}^{(V)}. \tag{28}$$

In the remaining part of this section, we first illustrate our solutions to the optimization problems (25) and (26). Then, we focus on the problem of selecting a proper value for $\tilde{I}$ and on the initialization of the proposed method.

1) WEIGHT EVALUATION

Subproblem (25) can be easily solved by means of the *Newton method* [27], [36]. Since the cost function $e(\mathbf{b}, \mathbf{h})$ (18) exhibits a *quadratic* dependence on $\mathbf{b}$, the convergence of this method in a single iteration is guaranteed for an arbitrary $\mathbf{h}^{(v-1)}$ and $\tilde{\mathbf{b}}$. Then, the solution to (25) can be expressed as

$$\mathbf{b}^{(v)} = \tilde{\mathbf{b}} - \mathbf{g}(\tilde{\mathbf{b}}, \mathbf{h}^{(v-1)})\mathbf{H}^{-1}(\mathbf{h}^{(v-1)}), \tag{29}$$

where

$$\mathbf{g}(\mathbf{b}, \mathbf{h}) = -\frac{2}{K}\left(\mathbf{v}^{\circ 2} \odot \left(\mathbf{p}^{(\mathrm{D})} - \mathbf{p}^{(\mathrm{L})}(\mathbf{b}, \mathbf{h})\right)\right)^{T} \mathbf{P}(\mathbf{h}) \tag{30}$$

and

$$\mathbf{H}(\mathbf{h}) = \frac{2}{K}\left(\left(\mathbf{v}^{\circ 2}\mathbf{1}_{1,I}\right) \odot \mathbf{P}(\mathbf{h})\right)^{T} \mathbf{P}(\mathbf{h}) \tag{31}$$

represent the I-dimensional gradient and the $I \times I$ Hessian, respectively, of $e(\mathbf{b}, \mathbf{h})$ (18) (both are evaluated with respect to $\mathbf{b}$).

2) SHIFT EVALUATION

Subproblem (26) is also solved by applying the Newton method; however, in this case, multiple iterations of it could be required to get an accurate approximation of its solution. The w th iteration of the resulting algorithm, accomplished within the vth iteration of the SWSUP method (with $w = 1, 2, \ldots, W$, where W denotes the overall number of iterations) can be expressed as

$$\mathbf{h}_v^{(w)} = \mathbf{h}_v^{(w-1)} - \dot{\mathbf{e}}(\mathbf{b}^{(v)}, \mathbf{h}_v^{(w-1)}) \oslash \ddot{\mathbf{e}}(\mathbf{b}^{(v)}, \mathbf{h}_v^{(w-1)}); \tag{32}$$

here,

$$\dot{\mathbf{e}}(\mathbf{b}, \mathbf{h}) = -\frac{2}{K}\mathbf{b} \odot \left(\left(\mathbf{v}^{\circ 2} \odot (\mathbf{p}^{(\mathrm{D})} - \mathbf{p}^{(\mathrm{L})}(\mathbf{b}, \mathbf{h}))\right)^{T} \dot{\mathbf{P}}(\mathbf{h})\right), \tag{33}$$

and

$$\begin{aligned}\ddot{\mathbf{e}}(\mathbf{b}, \mathbf{h}) = \frac{2}{K}\Bigg(&\mathbf{b}^{\circ 2} \odot \left(\mathbf{1}_{1,K}((\mathbf{v}^{\circ 2}\mathbf{1}_{1,I}) \odot \dot{\mathbf{P}}^{\circ 2}(\mathbf{h}))\right) \\ &- \mathbf{b} \odot \left(\left(\mathbf{v}^{\circ 2} \odot (\mathbf{p}^{(\mathrm{D})} - \mathbf{p}^{(\mathrm{L})}(\mathbf{b}, \mathbf{h}))\right)^{T} \ddot{\mathbf{P}}(\mathbf{h})\right)\Bigg),\end{aligned} \tag{34}$$

represent $\tilde{I}$-dimensional vectors collecting the first order and the second order derivatives, respectively, of $e(\mathbf{b}, \mathbf{h})$ (18) evaluated with respect to $\mathbf{h}$; moreover, $\dot{\mathbf{P}} = [\dot{P}_{k,l}]$ is a $K \times I$ matrix, with

$$\begin{aligned}\dot{P}_{k,l} \triangleq \left.\frac{\partial P^{(\mathrm{S})}(\gamma, \eta)}{\partial \eta}\right|_{\gamma=\gamma_k, \eta=\eta_l} = \frac{\pi}{M^2}\frac{\sin\left(\frac{M\pi}{2}(\gamma_k - \eta_l)\right)}{\sin^3\left(\frac{\pi}{2}(\gamma_k - \eta_l)\right)} \\ \left[\cos\left(\frac{\pi}{2}(\gamma_k - \eta_l)\right)\sin\left(\frac{M\pi}{2}(\gamma_k - \eta_l)\right)\right. \\ \left. - M\cos\left(\frac{M\pi}{2}(\gamma_k - \eta_l)\right)\sin\left(\frac{\pi}{2}(\gamma_k - \eta_l)\right)\right]\end{aligned} \tag{35}$$

and $\ddot{\mathbf{P}}(\mathbf{h}) = [\ddot{P}_{k,l}]$ is a $K \times I$ matrix, with

$$\begin{aligned}\ddot{P}_{k,l} \triangleq \left.\frac{\partial^2 P(\gamma, \eta)}{\partial \eta^2}\right|_{\gamma=\gamma_k, \eta=\eta_l} = \frac{\pi^2}{M^2\sin^4\left(\frac{\pi}{2}(\gamma_k - \eta_l)\right)} \\ \left[\frac{M^2}{2}\left(\cos^2\left(\frac{M\pi}{2}(\gamma_k - \eta_l)\right)\sin^2\left(\frac{\pi}{2}(\gamma_k - \eta_l)\right)\right.\right. \\ \left. - \sin^2\left(\frac{M\pi}{2}(\gamma_k - \eta_l)\right)\sin^2\left(\frac{\pi}{2}(\gamma_k - \eta_l)\right)\right) \\ - \frac{M}{2}\sin\left(M\pi(\gamma_k - \eta_l)\right)\sin\left(\pi(\gamma_k - \eta_l)\right) \\ + \frac{1}{2}\sin^2\left(\frac{M\pi}{2}(\gamma_k - \eta_l)\right)\left(\sin^2\left(\frac{\pi}{2}(\gamma_k - \eta_l)\right)\right. \\ \left.\left. + 3\cos^2\left(\frac{\pi}{2}(\gamma_k - \eta_l)\right)\right)\right].\end{aligned} \tag{36}$$

The iterative procedure expressed by (32) is initialized by setting $\mathbf{h}_v^{(0)} = \mathbf{h}^{(v-1)}$ and is repeated W times. At the end of the last iteration the output is generated setting $\mathbf{h}^{(v)} = \mathbf{h}_v^{(W)}$.

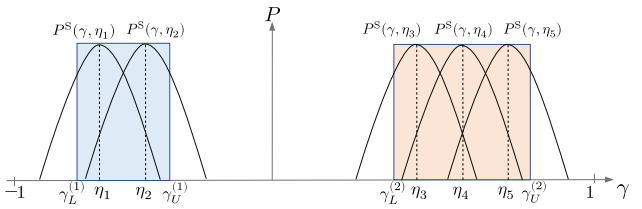

FIGURE 3. Representation of the shape of a desired asymmetric multilobe beampattern and of that of five components employed to approximate it; in this case, $N_L = 2$, $D^{(1)} = 2$ and $D^{(2)} = 3$ have been selected.

3) INITIALIZATION

Let us take into consideration now the following two problems: a) how to initialize the SWSUP method (i.e., how to select $\mathbf{h}^{(0)}$); b) how to select a proper value for the number of components $\tilde{I}$. Let assume that the desired beampattern $P^{(\mathrm{D})}(\gamma)$ has N_L lobes, i.e., that $P^{(\mathrm{D})}(\gamma) = 1$ for

$$\gamma \in \left[\gamma_L^{(1)}, \gamma_U^{(1)}\right] \cup \left[\gamma_L^{(2)}, \gamma_U^{(2)}\right] \ldots \cup \left[\gamma_L^{(N_L)}, \gamma_U^{(N_L)}\right] \quad (37)$$

and $P^{(\mathrm{D})}(\gamma) = 0$ otherwise; here, $\gamma_L^{(l)}$ and $\gamma_U^{(l)}$ represent the lower limit and the upper limit, respectively, of the lth lobe (with $l = 1, 2, \ldots, N_L$). Our solution to problem a) is based on the idea of approximating the lth lobe of the desired beampattern through the combination of $D^{(l)}$ *equally spaced* components, each obtained by introducing a proper shift in $P^{(\mathrm{S})}(\gamma, \eta)$ (16). In practice, to initialise the SWSUP method, the (initial) shifts for the first and the last component are selected as

$$\eta_1^{(l)} = \gamma_L^{(l)} + \frac{1}{M} \quad (38)$$

and

$$\eta_{D^{(l)}}^{(l)} = \gamma_U^{(l)} - \frac{1}{M}, \quad (39)$$

respectively, for any l; moreover, $D^{(l)}$ is evaluated as[6]

$$D^{(l)} = \left\lceil \left(\gamma_U^{(l)} - \gamma_L^{(l)}\right) \frac{M}{2} \right\rceil + 1, \quad (40)$$

for any l. The application of the selection strategy described above is exemplified by Fig. 3, where the use of shifted beampatterns for approximating a desired beampattern having two mainlobes of different widths is shown.

Based on our previous choices, the total number $\tilde{I}$ of components required to build the desired beampattern (including all the mainlobes) is selected as

$$\tilde{I} = I \triangleq \sum_{l=1}^{N_L} D^{(l)}, \quad (41)$$

where $D^{(l)}$ is expressed by (40). This solves problem b) and concludes our description of the SWSUP method, which is summarized in Algorithm 1.

[6]Note that $D^{(l)}$ is proportional to the width of the lth mainlobe and to the overall number of available antennas.

Algorithm 1 SWSUP Method

Input: desired beampattern $P^{(\mathrm{D})}(\gamma)$, directions of interest $\{\gamma_k\}$, overall number of TX antennas M, weights $\{\omega_k\}$.
Weight evaluation initialization:
Compute $\mathbf{p}^{(\mathrm{D})} = [P^{(\mathrm{D})}(\gamma_k)]$.
Set $\tilde{I}$, $\mathbf{h}^{(0)}$ (see Subsection III-B3).
Select $\tilde{\mathbf{b}}$ arbitrarily.
Evaluate $\mathbf{P}(\mathbf{h}^{(0)})$ (see (21)).
Begin weight evaluation:
for $v = 1, 2, \ldots, V$ **do**
  Evaluate the vector $\mathbf{p}^{(\mathrm{L})}(\tilde{\mathbf{b}}, \mathbf{h}^{(v-1)})$ according to (20).
  Evaluate the vector $\mathbf{g}(\tilde{\mathbf{b}}, \mathbf{h}^{(v-1)})$ according to (30).
  Evaluate the vector $\mathbf{H}(\mathbf{h}^{(v-1)})$ according to (31).
  Evaluate the vector $\mathbf{b}^{(v)}$ according to (29).
  Shift evaluation initialization:
  $\mathbf{h}_v^{(0)} = \mathbf{h}^{(v-1)}$
  for $w = 1, 2, \ldots, W$ **do**
    Evaluate the vector $\dot{\mathbf{e}}(\mathbf{h}_v^{(w-1)}, \mathbf{b}^{(v)})$ according to (33).
    Evaluate the vector $\ddot{\mathbf{e}}(\mathbf{h}_v^{(w-1)}, \mathbf{b}^{(v)})$ according to (34).
    Evaluate the vector $\mathbf{h}_v^{(w)}$ according to (32).
    Update the matrix $\mathbf{P}(\mathbf{h}_v^{(w)}) = [P_{k,l}]$ (see (21)).
  end for
  Set $\mathbf{h}^{(v)} = \mathbf{h}_v^{(W)}$
  End shift evaluation
end for
Set $\hat{\mathbf{b}} = \mathbf{b}^{(V)}$
Set $\hat{\mathbf{h}} = \mathbf{h}^{(V)}$
End weight evaluation
Evaluate the matrix $\hat{\mathbf{R}}^{(\mathrm{L})}$ according to (23).
Output: $\hat{\mathbf{R}}^{(\mathrm{L})}$

C. COMPARISON WITH OTHER METHODS

Let us compare now the SWSUP method with other related alternatives available in the technical literature; in particular, we focus on other methods that aim at the minimization of the MSE between the desired transmit beampattern and the synthesized one, namely the *Semi-Definite Quadratic Programming* (SQP), *Uniform phase array Library* (UPA-LIB) and ADMM methods (such methods have been developed in [29] and [30], respectively). The main differences among all these methods can be summarized as follows. On the one hand, the SWSUP, SQP and UPA-LIB methods aim at computing the signal covariance matrix; on the other hand, the ADMM method synthesizes the transmitted waveforms directly. Moreover, the SQP and UPA-LIB methods require the use of a toolbox for solving constrained optimization problems (e.g., CVX); the SWSUP method, instead, being *unconstrained* , minimizes the MSE through a much simpler procedure. For this reason, the SWSUP method is much faster than all the other aforementioned alternatives; despite this, as shown in the next section, it achieves similar performance in terms of MSE. The complexity of the SWSUP method

TABLE 1. Order of the computational complexity of the UPA-LIB, SQP, ADMM and SWSUP methods.

Method	Complexity order
UPA-LIB	$\mathcal{O}(M^2 + KM^{1.18})$
SQP	$\mathcal{O}(KM^{3.5})$
ADMM*	$\mathcal{O}(2(KM^2N^2 + M^3N^3))$
SWSUP**	$\mathcal{O}(50WKM + KM^2 + M^{2.373})$

* This estimate refers to a single iteration of the ADMM method.
**This estimate refers to a single iteration of the weight evaluation algorithm.

can be assessed by summing that of the weight evaluation algorithm with that of the shift evaluation algorithm (see Subsubsections III-B1 and III-B2, respectively). The computational complexity of the single iteration of the first algorithm is $\mathcal{O}(M^{2.373} + KM^2)$; the main contributions to it are due to the matrix multiplication in (31) and to the matrix inversion in (29); these account for $\mathcal{O}(KM^2)$ and $\mathcal{O}(M^{2.373})$ [37], respectively. As far as the second algorithm is concerned, it can be shown that the computational cost of each of its iterations (see (32) is $\mathcal{O}(50KM)$; this result originates from the assessment of the complexity of (35) and (36). Further details about the complexity of the SWSUP method can be found in Appendix B. The order of the overall complutational complexity of the SWSUP method and that of the other three methods considered in this manuscript are listed in Table 1. The formulas appearing in this table deserve the following comments (that are useful in the interpretation of the results illustrated in the next section):

1) The expression of the complexity order of each method unveils how the corresponding computing time scales with respect to the involved parameters (e.g., M and K). However, we should never forget that the computing times of different methods should not be compared on the basis of their the complexity orders, since such times are significantly influenced by the specifications of the machine on which the considered methods are run.

2) For this reason, even if the complexity order of the UPA-LIB method appears lower than that of the other methods, this does not necessarily imply that the corresponding computing time will be shorter for the same values of the parameters M and K.

3) The considered methods exhibit a different dependence on the array size (i.e., on M). In particular, the computational cost of the SWSUP method is proportional to $M^{2.373}$; as it can be easily inferred from Table 1, only the UPA-LIB method exhibits a weaker dependence on M. However, for reasonable values of M and K (say, in the order of few thousands), the dominant term in the complexity order of the SWSUP method is $\mathcal{O}(50WKM)$, i.e. the term exhibiting a linear dependence on M. In contrast, the computing time of the UPA-LIB method depends quadratically on M.

4) As evidenced by our computer simulations, the SWSUP method requires the shortest computing time if M is less than a few thousands; this is due to the fact that the computational cost of each iteration is small.

IV. NUMERICAL RESULTS

In this section, we take into consideration a couple of specific applications of the SWSUP method and of the related methods mentioned in Subsection III-C, and compare them in terms of MSE and computing time; the values provided for the last parameter refer to the *personal computer* (PC) on which our simulations have been run (namely, a PC equipped with a) 32 GB RAM and b) a 64-bit Intel i7 − 12700 CPU running at 2.10 GHz). In our computer simulations, we have assumed that the available TX ULA consists of $M = 30$ and that the total power it radiates is $\rho = 1$ (see (6)). In all cases, the evaluation of the MSE (18) involves, unless differently stated, $K = 2001$ uniformly spaces values of γ ranging from -1 to 1 (i.e., ranging from -90° to 90° in the θ domain; see (7)). Moreover, the following specific choices have been made for the parameters of the considered methods:

1. SWSUP method - A unit value has been assigned to all the elements of the vector $\mathbf{v}$ (22). Moreover, two different cases have been considered for the values of the parameters V and W. In the first case $V = 1$ and $W = 0$ are selected, so that only weight evaluation is performed. The second case, instead, is characterized by $V = 10$ and $W = 90$, so that both weights and shifts are iteratively refined.

2. ADMM method - Ten samples (i.e., $N = 10$) have been taken in the synthesis of the radiated waveforms.

It is also important to keep in mind that:

1. The SQP and UPA-LIB methods exploit the CVX toolbox; the termination criteria and number of iterations required to reach a given inner threshold are determined internally by the package, to which we do not have direct access.

2. Based on our knowledge, we can state that the termination criteria of the ADMM method are met after 15 iterations.

In our analysis of beampattern design, two different cases have been taken into consideration. In the first case, the desired beampattern has a singlelobe and is such that $P^{(\mathrm{D})}(\gamma) = 1$ for $\gamma \in [-0.5, 0.5]$ (or equivalently $\theta \in [-30°, 30°]$). In the second case, instead, a multilobe asymmetric beampattern is assumed; more specifically, the desired beampattern has three mainlobes, and is such that $P^{\mathrm{D}}(\theta) = 1$ for $\theta \in [-50°, -40°] \cup [-15°, 15°] \cup [40°, 60°]$. The desired beampattern and those synthesized through the four considered methods are shown in Figs. 4 and 5 for the first and the second case, respectively. Moreover, the MSEs achieved by the considered methods and their computing time are listed in Tables 2 and 3 for the first and the second case, respectively.

From these results the following conclusions can be easily inferred:

1) The MSE achieved by the SWSUP method is very close to that characterizing the other methods (and, in particular, the SQP method) even when weight evaluation only is accomplished (i.e., when $V = 1$ and $W = 0$ are selected).

2) In the case of singlelobe beampattern, the computing time required by the SWSUP method in the case of weight

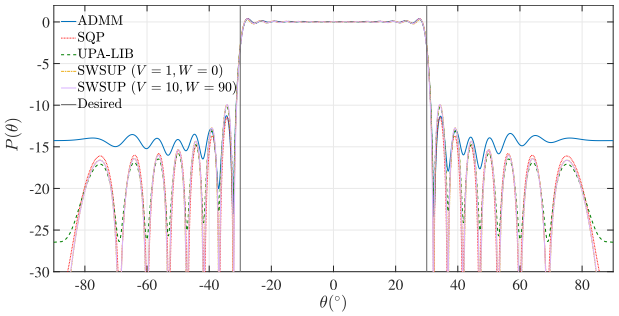

FIGURE 4. Representation of: 1) a desired beampattern characterized by a singlelobe (delimited by black vertical lines); b) the beampatterns synthesized through the considered design methods.

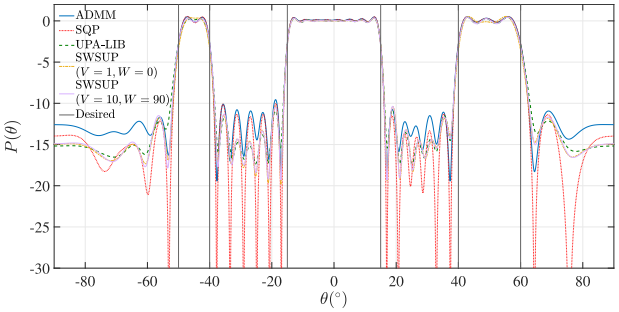

FIGURE 5. Representation of: 1) a desired beampattern characterized by multiple lobes (delimited by black vertical lines); 2) the beampatterns synthesized through the considered design methods.

TABLE 2. Comparison of various beampattern design methods in terms of computing time and MSE. The corresponding beampatterns are shown in Fig. 4.

Method	Time (s)	MSE
UPA-LIB	0.73	0.00394
SQP	7.7	0.00383
ADMM	155	0.00405
SWSUP(V=1,W=0)	0.0004	0.00394
SWSUP(V=5,W=10)	0.06	0.00387
SWSUP(V=10,W=90)	1.07	0.00386

TABLE 3. Comparison of various beampattern design methods in terms of computing time and MSE. The corresponding beampatterns are shown in Fig. 5.

Method	Time (s)	MSE
UPA-LIB	0.74	0.0129
SQP	7.9	0.0114
ADMM	151	0.012
SWSUP(V=1,W=0)	0.0004	0.0129
SWSUP(V=5,W=10)	0.05	0.0121
SWSUP(V=10,W=90)	0.92	0.012

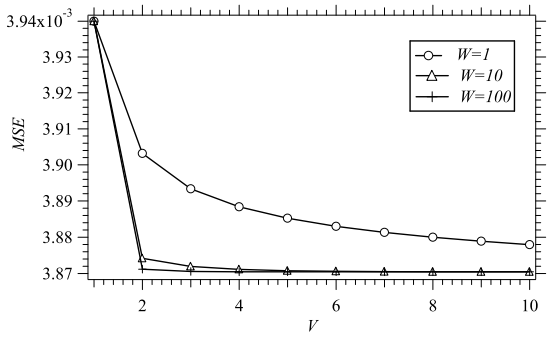

FIGURE 6. Representation of the SWSUP MSE on V; three different values of W are considered.

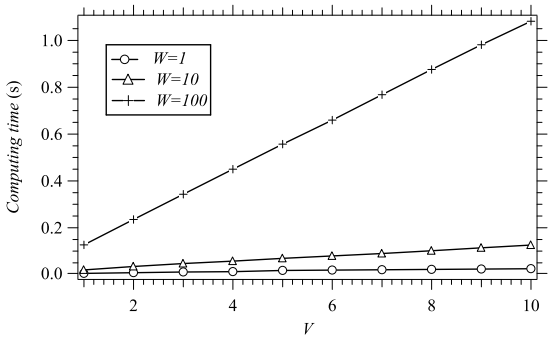

FIGURE 7. Representation of the SWSUP computing time on V; three different values of W are considered.

evaluation only is 1800, 19000 and 380000 times faster than that characterizing the UPA-LIB, SQP and ADMM methods, respectively; the price to be paid is a 3% increase in the resulting MSE.

3) In the case of multilobe beampattern, the MSE achieved by the the SWSUP method, in the case of weight evaluation only, is approximately 10% higher than that provided by the other methods. However, the SWSUP method is 1800, 19000 and 370000 times faster than the UPA-LIB, SQP and ADMM methods, respectively. A small reduction (approximately 6%) in the resulting MSE is obtained if both weight evaluation and shift evaluation are carried out in the SWSUP method. However, in this case, the computing time increases by 800 times; despite this, the computing time characterizing the SWSUP method remains substantially lower than that observed for all the other methods.

Further results about the SWSUP method are offered in Fig. 6 and Fig. 7, in which the dependence of the achieved MSE and computing time, respectively, on V is represented for three different values of W (namely, $W = 1$, 10 and 100) when synthetizing a centered beampattern spanning from $-30°$ to $30°$. These results show that:

1) The dependence of the achieved accuracy on V and especially on W is weak, and convergence is obtained with few iterations.

2) In the considered case, $V = 5$ and $W = 10$ are enough to closely approach the MSE floor. The adoption of higher values for V and W (e.g., $V = 10$ and $W = 90$) provides a minor improvement in terms of MSE at the price of a significantly longer computational time.

Further insights into the SWSUP method are provided by the numerical results collected in Table 4 and Table 5; these

TABLE 4. Comparison of various design methods in terms of average MSE and computing time evaluated over 100 random singlelobe beampatterns.

Method	Mean (MSE)	Std (MSE)	Mean (Time (s))	Std (Time (s))
UPA-LIB	0.00424	1.55e-4	1.13	0.35
SQP	**0.00382**	1.22e-4	7.41	0.96
ADMM	0.00409	1.50e-4	152.3	1.26
SWSUP(V=1,W=0)	0.00420	1.25e-4	2.84e-4	9e-5
SWSUP(V=5,W=10)	0.00403	8.21e-5	0.065	2.07e-2
SWSUP(V=10,W=90)	**0.00384**	1.13e-4	1.21	0.42

TABLE 5. Comparison of various design methods in terms of average MSE and computing time evaluated over 100 random multilobe beampatterns.

Method	Mean (MSE)	Std (MSE)	Mean (Time (s))	Std (Time (s))
UPA-LIB	0.0086	3.55e-4	1.415	0.32
SQP	**0.0079**	5.26e-4	7.78	0.66
ADMM	0.0089	4.71e-4	143.8	1.21
SWSUP(V=1,W=0)	0.0086	5.69e-4	2.47e-4	9.6e-5
SWSUP(V=5,W=10)	0.0082	2.97e-4	0.05	1.75e-2
SWSUP(V=10,W=90)	**0.0079**	2.44e-4	1.015	0.31

results refer to a) the average MSE and its standard deviation (Std), and b) the average computing time characterizing the SWSUP method when it is applied to one hundred randomly generated singlelobe and multilobe beampatterns (see Table 4 and Table 5, respectively).[7] In both scenarios, the accuracy of the SWSUP method has been assessed in the following two cases: 1) when weights only are evaluated (i.e., for $V = 1$ and $W = 0$); 2) when both weights and shifts are computed ($V = 5$, $W = 10$ and $V = 10$, $W = 90$ have been selected in this case). These results lead to the conclusion that, in the first case, the SWSUP method is able to achieve an acceptable MSE in a significantly shorter time than the other methods. Moreover, the improvement obtained in the second case makes the accuracy of the SWSUP method very close to that of the SQP method. Note also that, despite the large values selected for both V and W in the second case, the SWSUP method still requires a significantly smaller computational effort than its alternatives; for instance, on the average, it is 6.12 times and 7.6 times faster than the SQP method in singlelobe scenarios and in multilobe scenarios, respectively.

Finally, it is important to point out that the the covariance matrices generated by the considered methods can be substantially different. This is exemplified by Fig. 8, in which the absolute value of the elements of the covariance matrix generated by each method for the beampattern shown in Fig. 5 is represented through a colour map.[8] Note that all the represented matrices are PSD and have identical diagonal elements, i.e. satisfy typical constraints.

[7] In the singlelobe scenario, $\gamma_L^{(1)}$ and $\gamma_U^{(1)}$ have been randomly selected in the intervals $[-80°, -5°]$ and $[5°, 80°]$, respectively; in the multilobe scenario, instead, we have randomly selected $\gamma_U^{(1)}$, $\gamma_L^{(1)}$, $\gamma_L^{(2)}$ and $\gamma_U^{(2)}$ in the intervals $[-40°, 0°]$, $[-80°, \gamma_U^{(1)} - 5°]$, $[0°, 40°]$ and $[\gamma_L^{(2)} + 5°, 80°]$, respectively (see Fig. 3).

[8] Note that covariance matrix for the ADMM method has been computed on the basis of the waveforms it produces.

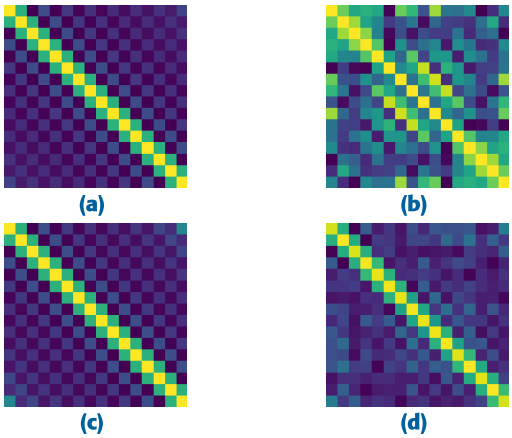

FIGURE 8. Colour maps representing the absolute value of the elements of the covariance matrix generated by: a) the SWSUP method; b) the SQP method; c) the UPA-LIB method; d) the ADMM method.

V. CONCLUSION

In this manuscript, a novel solution to the problem of beampattern matching design for colocated MIMO radars has been developed. This solution is based on the idea of synthesizing the covariance matrix of the radiated signals by superimposing multiple shifted and weighted replicas of a proper basis covariance matrix. This representation leads to formulating the beampattern matching design as an optimization problem that can be tackled by exploiting alternating minimization and the Newton method. The resulting solution is accurate and much faster than all the other related methods available in the technical literature. This makes it useful for real-time applications, particularly in scenarios in which swift beamforming is required, especially in the presence of large antenna arrays. Our future work concerns the extension of the proposed approach to other geometries of the radar array.

APPENDIX A DERIVATION OF THE BASIS BEAMPATTERN

In this Appendix, the derivation of (16) is sketched. To begin, substituting the *right-hand side* (RHS) of (15) in that of (12) yields

$$\begin{aligned} P^{(\mathrm{S})}(\gamma,\eta) &= \sum_{m=0}^{M-1} e^{-j\pi m(\gamma-\eta)} \sum_{m=0}^{M-1} e^{j\pi m(\gamma-\eta)} \\ &= \frac{1-e^{-j\pi M(\gamma-\eta)}}{1-e^{-j\pi(\gamma-\eta)}} \frac{1-e^{j\pi M(\gamma-\eta)}}{1-e^{j\pi(\gamma-\eta)}} \\ &= \frac{1-\cos(\pi M(\gamma-\eta))}{1-\cos(\pi(\gamma-\eta))} \end{aligned}$$

The last formula can be easily rewritten in the form (16), thanks to the fact that $1-\cos(2x) = 2\sin^2(x)$ for any x.

APPENDIX B EVALUATION OF THE COMPUTATIONAL COMPLEXITY OF THE SWSUP METHOD

In this Appendix, the overall complexity *order* $\mathcal{O}_{SWSUP}$ of the SWSUP method is assessed. This order can be expressed as

$$\mathcal{O}_{SWSUP} = V(\mathcal{O}_w + W\mathcal{O}_s) \tag{42}$$

where $\mathcal{O}_w$ ($\mathcal{O}_s$) and V (W) represent the overall number of iterations carried out for weight (shift) evaluation and the complexity order of a single iteration, respectively. The general criteria adopted in estimating the computational costs that appear in the RHS of (42) are illustrated in [38] and can be summarised as follows:

- the order of the multiplication between a $(n \times m)$ matrix and a $(m \times p)$ matrix is $\mathcal{O}(nmp)$;
- the order of the inversion of a $(n \times n)$ matrix is $\mathcal{O}(n^{2.373})$;
- all the other operations grow linearly with the input size.

The order $\mathcal{O}_w$ (see (25)) can be expressed as

$$\mathcal{O}_w = \mathcal{O}_{\mathbf{b}} + \mathcal{O}_{\mathbf{g}} + \mathcal{O}_{\mathbf{H}}, \tag{43}$$

where $\mathcal{O}_{\mathbf{b}} = \mathcal{O}(I^{2.373} + I^2 + I)$, $\mathcal{O}_{\mathbf{g}} = \mathcal{O}(3K + I + KI)$ and $\mathcal{O}_{\mathbf{H}} = \mathcal{O}(K + 2KI + KI^2 + I^2)$ represent the contributions due to (29), (30) and (31), respectively. Consequently, we have that

$$\mathcal{O}_w = \mathcal{O}(I^{2.373} + KI^2 + 3KI + 4K + 2I^2 + 2I). \tag{44}$$

Similarly, the order $\mathcal{O}_s$ (see 26) can be expressed as

$$\mathcal{O}_s = \mathcal{O}_{\mathbf{h}} + \mathcal{O}_{\dot{\mathbf{e}}} + \mathcal{O}_{\dot{\mathbf{P}}} + \mathcal{O}_{\ddot{\mathbf{e}}} + \mathcal{O}_{\ddot{\mathbf{P}}}, \tag{45}$$

where $\mathcal{O}_{\mathbf{h}} = \mathcal{O}(2I)$, $\mathcal{O}_{\dot{\mathbf{e}}} = \mathcal{O}(3K + KI + 2I)$, $\mathcal{O}_{\dot{\mathbf{P}}} = \mathcal{O}(15KI)$, $\mathcal{O}_{\ddot{\mathbf{e}}} = \mathcal{O}(3K + 5KI + 5I)$ and $\mathcal{O}_{\ddot{\mathbf{P}}} = \mathcal{O}(29KI)$ represent the contributions due to (32), (33), (35), (34) and (36), respectively. Then, we have that

$$\mathcal{O}_s = \mathcal{O}(6K + 50KI + 9I). \tag{46}$$

Substituting the RHS of (43) and (46) in that of (42) yields

$$\begin{aligned} \mathcal{O}_{SWSUP} = \mathcal{O}(V(&I^{2.373} + KI^2 + 3KI + 4K + 2I^2 + 2I \\ &+ W(6K + 50KI + 9I))) \end{aligned} \tag{47}$$

Finally, we note that the expression appearing in Table 1 is easily obtained from (47) by keeping their most relevant terms only (note also that I is upper bounded by M; see (40) and (41)).

REFERENCES

[1] J. Li and P. Stoica, *MIMO Radar Signal Processing* . Hoboken, NJ, USA: Wiley, 2008.

[2] L. Xu, J. Li, and P. Stoica, "Target detection and parameter estimation for MIMO radar systems," *IEEE Trans. Aerosp. Electron. Syst.* , vol. 44, no. 3, pp. 927–939, Jul. 2008.

[3] A. Hassanien and S. A. Vorobyov, "Phased-MIMO radar: A tradeoff between phased-array and MIMO radars," *IEEE Trans. Signal Process.* , vol. 58, no. 6, pp. 3137–3151, Jun. 2010.

[4] Z. Cheng, Z. He, B. Liao, and M. Fang, "MIMO radar waveform design with PAPR and similarity constraints," *IEEE Trans. Signal Process.* , vol. 66, no. 4, pp. 968–981, Feb. 2018.

[5] X. Yu, K. Alhujaili, G. Cui, and V. Monga, "MIMO radar waveform design in the presence of multiple targets and practical constraints," *IEEE Trans. Signal Process.* , vol. 68, pp. 1974–1989, 2020.

[6] X. Yu, G. Cui, J. Yang, and L. Kong, "MIMO radar transmit–receive design for moving target detection in signal-dependent clutter," *IEEE Trans. Veh. Technol.* , vol. 69, no. 1, pp. 522–536, Jan. 2020.

[7] M. Bolhasani, E. Mehrshahi, S. A. Ghorashi, and M. S. Alijani, "Constant envelope waveform design to increase range resolution and SINR in correlated MIMO radar," *Signal Process.* , vol. 163, pp. 59–65, Oct. 2019.

[8] P. Stoica, J. Li, and X. Zhu, "Waveform synthesis for diversity-based transmit beampattern design," *IEEE Trans. Signal Process.* , vol. 56, no. 6, pp. 2593–2598, Jun. 2008.

[9] Z.-F. Cheng, Y.-B. Zhao, H. Li, and P.-L. Shui, "Sparse representation framework for MIMO radar transmit beampattern matching design," *IEEE Trans. Aerosp. Electron. Syst.* , vol. 53, no. 1, pp. 520–529, Feb. 2017.

[10] X. Zhang, Z. He, L. Rayman-Bacchus, and J. Yan, "MIMO radar transmit beampattern matching design," *IEEE Trans. Signal Process.* , vol. 63, no. 8, pp. 2049–2056, Apr. 2015.

[11] I. Mallioras, T. V. Yioultsis, N. V. Kantartzis, P. I. Lazaridis, A. Vlahov, V. Poulkov, and Z. D. Zaharis, "Zero forcing beamforming with sidelobe suppression using neural networks," in *Proc. 28th Eur. Wireless Conf. Eur. Wireless* , Oct. 2023, pp. 203–208.

[12] I. P. Gravas, Z. D. Zaharis, T. V. Yioultsis, P. I. Lazaridis, and T. D. Xenos, "Adaptive beamforming with sidelobe suppression by placing extra radiation pattern nulls," *IEEE Trans. Antennas Propag.* , vol. 67, no. 6, pp. 3853–3862, Jun. 2019.

[13] S. Imani and M. M. Nayebi, "A coordinate descent framework for beampattern design and waveform synthesis in MIMO radars," *IEEE Trans. Aerosp. Electron. Syst.* , vol. 57, no. 6, pp. 3552–3562, Dec. 2021.

[14] S. Ahmed and M. Alouini, "A survey of correlated waveform design for multifunction software radar," *IEEE Aerosp. Electron. Syst. Mag.* , vol. 31, no. 3, pp. 19–31, Mar. 2016.

[15] S. Ahmed, John. S. Thompson, Y. R. Petillot, and B. Mulgrew, "Finite alphabet constant-envelope waveform design for MIMO radar," *IEEE Trans. Signal Process.* , vol. 59, no. 11, pp. 5326–5337, Nov. 2011.

[16] S. Ahmed and M.-S. Alouini, "MIMO radar transmit beampattern design without synthesising the covariance matrix," *IEEE Trans. Signal Process.* , vol. 62, no. 9, pp. 2278–2289, May 2014.

[17] S. Imani, M. Bolhasani, S. A. Ghorashi, and M. Rashid, "Waveform design in MIMO radar using radial point interpolation method," *IEEE Commun. Lett.* , vol. 22, no. 10, pp. 2076–2079, Oct. 2018.

[18] H. Deng, Z. Geng, and B. Himed, "MIMO radar waveform design for transmit beamforming and orthogonality," *IEEE Trans. Aerosp. Electron. Syst.* , vol. 52, no. 3, pp. 1421–1433, Jun. 2016.

[19] M. Deng, Z. Cheng, X. Lu, and Z. He, "Binary waveform design for MIMO radar with good transmit beampattern performance," *Electron. Lett.* , vol. 55, no. 19, pp. 1061–1063, Sep. 2019.

[20] W. Zhang, J. Hu, Z. Wei, H. Ma, X. Yu, and H. Li, "Constant modulus waveform design for MIMO radar transmit beampattern with residual network," *Signal Process.* , vol. 177, Dec. 2020, Art. no. 107735.

[21] H. Al Kassir, N. V. Kantartzis, P. I. Lazaridis, P. Sarigiannidis, S. K. Goudos, C. G. Christodoulou, and Z. D. Zaharis, "Improving DOA estimation via an optimal deep residual neural network classifier on uniform linear arrays," *IEEE Open J. Antennas Propag.* , vol. 5, pp. 460–473, 2024.

[22] W. Fan, J. Liang, and J. Li, "Constant modulus MIMO radar waveform design with minimum peak sidelobe transmit beampattern," *IEEE Trans. Signal Process.* , vol. 66, no. 16, pp. 4207–4222, Aug. 2018.
[23] Z. Cheng, Z. He, S. Zhang, and J. Li, "Constant modulus waveform design for MIMO radar transmit beampattern," *IEEE Trans. Signal Process.* , vol. 65, no. 18, pp. 4912–4923, Sep. 2017.
[24] Y. Liu, B. Jiu, and H. Liu, "ADMM-based transmit beampattern synthesis for antenna arrays under a constant modulus constraint," *Signal Process.* , vol. 171, Jun. 2020, Art. no. 107529.
[25] J. Liang, H. C. So, J. Li, and A. Farina, "Unimodular sequence design based on alternating direction method of multipliers," *IEEE Trans. Signal Process.* , vol. 64, no. 20, pp. 5367–5381, Oct. 2016.
[26] W. Fan, J. Liang, G. Lu, X. Fan, and H. C. So, "Spectrally-agile waveform design for wideband MIMO radar transmit beampattern synthesis via majorization-ADMM," *IEEE Trans. Signal Process.* , vol. 69, pp. 1563–1578, 2021.
[27] S. Boyd and L. Vandenberghe, *Convex Optimization* . Cambridge, U.K.: Cambridge Univ. Press, 2004.
[28] M. Grant and S. Boyd. (2014). *CVX: Matlab Software for Disciplined Convex Programming, Version 2.1* . [Online]. Available: http://cvxr.com/cvx
[29] P. Stoica, J. Li, and Y. Xie, "On probing signal design for MIMO radar," *IEEE Trans. Signal Process.* , vol. 55, no. 8, pp. 4151–4161, Aug. 2007.
[30] E. Faghand, E. Mehrshahi, and S. A. Ghorashi, "Complexity reduction in beamforming of uniform array antennas for MIMO radars," *IEEE Trans. Radar Syst.* , vol. 1, pp. 413–422, 2023.
[31] P. Gong, Z. Shao, G. Tu, and Q. Chen, "Transmit beampattern design based on convex optimization for MIMO radar systems," *Signal Process.* , vol. 94, pp. 195–201, Jan. 2014.
[32] J. Lipor, S. Ahmed, and M.-S. Alouini, "Fourier-based transmit beampattern design using MIMO radar," *IEEE Trans. Signal Process.* , vol. 62, no. 9, pp. 2226–2235, May 2014.
[33] T. Bouchoucha, S. Ahmed, T. Al-Naffouri, and M.-S. Alouini, "DFT-based closed-form covariance matrix and direct waveforms design for MIMO radar to achieve desired beampatterns," *IEEE Trans. Signal Process.* , vol. 65, no. 8, pp. 2104–2113, Apr. 2017.
[34] X. Ai and L. Gan, "Beampattern matching in colocated MIMO radar using transmit covariance matrix design," *Signal Process.* , vol. 194, May 2022, Art. no. 108440.
[35] P. Stoica and R. Moses, *Spectral Analysis of Signals* . Upper Saddle River, NJ, USA: Prentice-Hall, 2005.
[36] C.-Y. Chi, W.-C. Li, and L. Chia-Hsiang, *Convex Optimization for Signal Processing and Communications* . Boca Raton, FL, USA: CRC Press, 2017.
[37] O. Aldayel, V. Monga, and M. Rangaswamy, "Tractable transmit MIMO beampattern design under a constant modulus constraint," *IEEE Trans. Signal Process.* , vol. 65, no. 10, pp. 2588–2599, May 2017.
[38] G. H. Golub and C. F. Van Loan, *Matrix Computations* , 3rd ed. Baltimore, MD, USA: Johns Hopkins Univ. Press, 1996.

ELAHE FAGHAND was born in Iran. She received the B.S. degree from Shahed University, in 2015, and the M.S. degree in electrical engineering from Shahid Beheshti University, Tehran, Iran, in 2018, where she is currently pursuing the Ph.D. degree with the Department of Electrical Engineering. She is a Visiting Researcher with the Department of Engineering "Enzo Ferrari," University of Modena and Reggio Emilia, Modena, Italy. Her research interests include millimeter-wave radars, signal processing methods for MIMO radars, ultrawideband radar imaging systems, and the design of radio frequency circuits.

GIORGIO GUERZONI received the B.S. and M.S. degrees (cum laude) in electronics engineering and the Ph.D. degree in information and communication technologies from the University of Modena and Reggio Emilia, Italy, in 2016, 2019, and 2023, respectively. His research interests include signal processing and machine learning methods for MIMO radars.

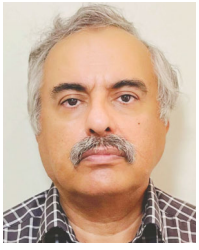

ESFANDIAR MEHRSHAHI received the B.Sc. degree in electrical engineering from Iran University of Science and Technology, Tehran, Iran, in 1987, and the M.Sc. and Ph.D. degrees in electrical engineering from the Sharif University of Technology, Tehran, in 1991 and 1998, respectively. Since 1990, he has been involved in several research and engineering projects with Iran Telecommunications Research Center (ITRC). He is currently an Associate Professor with Shahid Beheshti University (SBU), Tehran. His main areas of research interests include the nonlinear simulation of microwave circuits, low-phase noise oscillators, and computational electromagnetics.

GIORGIO MATTEO VITETTA (Senior Member, IEEE) received the Dr.-Ing. degree (cum laude) in electronic engineering and the Ph.D. degree from the University of Pisa, Italy, in 1990 and 1994, respectively. He has held the position of a Full Professor of telecommunications with the University of Modena and Reggio Emilia, since 2001. He has co-authored more than 100 papers published in international journals and on the proceedings of international conferences and has co-authored the book *Wireless Communications: Algorithmic Techniques* (John Wiley, 2013). His main research interests include wireless and wired data communications, localization systems, MIMO radars, and the smart grid. He has served as an Area Editor for IEEE TRANSACTIONS ON COMMUNICATIONS and as an Associate Editor for IEEE WIRELESS COMMUNICATIONS LETTERS and IEEE TRANSACTIONS ON WIRELESS COMMUNICATIONS.

SHOKROLLAH KARIMIAN is currently an Assistant Professor with the School of Electrical Engineering, Shahid Beheshti University, Tehran, Iran. He is a member of IET and EuMA and with over sixty publications, he has made a valuable contribution to the RF and microwave/mm-wave community.